

Article

The Synthesis and Evaluation of Aminocoumarin Peptidomimetics as Cytotoxic Agents on Model Bacterial *E. coli* Strains

Paweł Kowalczyk ^{1,*}, Monika Wilk ², Parul Parul ², Mateusz Szymczak ³, Karol Kramkowski ⁴,
Stanisława Raj ¹, Grzegorz Skiba ¹, Dorota Sulejczak ⁵, Patrycja Kleczkowska ^{6,7} and Ryszard Ostaszewski ^{2,*}

- ¹ Department of Animal Nutrition, The Kielanowski Institute of Animal Physiology and Nutrition, Polish Academy of Sciences, Instytutcka 3, 05-110 Jabłonna, Poland; s.raj@ifzz.pl (S.R.); g.skiba@ifzz.pl (G.S.)
² Institute of Organic Chemistry PAS, Kasprzaka 44/52, 01-224 Warsaw, Poland; monika.wilk@icho.edu.pl (M.W.); parul@icho.edu.pl (P.P.)
³ Department of Molecular Virology, Faculty of Biology, Institute of Microbiology, University of Warsaw, Miecznikowa 1, 02-096 Warsaw, Poland; mszymczak@biol.uw.edu.pl
⁴ Department of Physical Chemistry, Medical University of Białystok, Kilińskiego 1 Str., 15-089 Białystok, Poland; kkramk@wp.pl
⁵ Department of Experimental Pharmacology, Mossakowski Medical Research Institute, Polish Academy of Sciences, Pawinskiego 5, 02-106 Warsaw, Poland; dots@op.pl
⁶ Centre for Preclinical Research (CBP), Department of Pharmacodynamics, Medical University of Warsaw, Banacha 1B, 02-097 Warsaw, Poland; hazufiel@wp.pl
⁷ Military Institute of Hygiene and Epidemiology, Kozielska 4, 01-163 Warsaw, Poland
* Correspondence: p.kowalczyk@ifzz.pl (P.K.); rysard.ostaszewski@icho.edu.pl (R.O.)



Citation: Kowalczyk, P.; Wilk, M.; Parul, P.; Szymczak, M.; Kramkowski, K.; Raj, S.; Skiba, G.; Sulejczak, D.; Kleczkowska, P.; Ostaszewski, R. The Synthesis and Evaluation of Aminocoumarin Peptidomimetics as Cytotoxic Agents on Model Bacterial *E. coli* Strains. *Materials* **2021**, *14*, 5725. <https://doi.org/10.3390/ma14195725>

Academic Editor: John T. Kiwi

Received: 28 July 2021

Accepted: 26 September 2021

Published: 30 September 2021

Publisher's Note: MDPI stays neutral with regard to jurisdictional claims in published maps and institutional affiliations.



Copyright: © 2021 by the authors. Licensee MDPI, Basel, Switzerland. This article is an open access article distributed under the terms and conditions of the Creative Commons Attribution (CC BY) license (<https://creativecommons.org/licenses/by/4.0/>).

Abstract: This work presents the successful synthesis of a library of novel peptidomimetics via Ugi multicomponent reaction. Most of these peptidomimetics contain differently substituted aminocoumarin; 7-amino-4-methylcoumarin and 7-amino-4-(trifluoromethyl) coumarin. Inspired by the biological properties of coumarin derivatives and peptidomimetics, we proposed the synthesis of coumarin incorporated peptidomimetics. We studied the potential of synthesized compounds as antimicrobial drugs on model *E. coli* bacterial strains (k12 and R2–R4). To highlight the importance of coumarin in antimicrobial resistance, we also synthesized the structurally similar peptidomimetics, using benzylamine. Preliminary cellular studies suggest that the compounds with coumarin derivatives have more potential as antimicrobial agents compared to the compounds without coumarin. We also analyzed the effect of aldehyde, free acid group and ester group on the course of their antimicrobial properties.

Keywords: coumarin derivatives; DNA-N-glycosylase; Fpg protein-formamidopyrimidine; lipopolysaccharide (LPS); oxidative stress; Ugi multicomponent reaction

1. Introduction

Multi-component reactions have been accepted as potential substitutes for multistep organic synthesis. Ugi multicomponent reaction (MCR) is a four-component MCR, named after Ivar Ugi. It is a well-known Isocyanide-based MCR which requires aldehyde, amine, carboxylic acid and isocyanide to give α -acetoamido carboxymide derivative, also known as peptidomimetics. In this work, a Ugi reaction was successfully applied to the synthesis of coumarin peptidomimetics, the main bioactive components of which are the 7-amino-4-methylcoumarin and 7-amino-4-(trifluoromethyl) coumarin [1]. These compounds were initially found in cinnamon-flavored food [2,3] and used later for biological studies [4–9]. Moreover, coumarin derivatives have been used broadly in oncological medicine [10–14] and microbiology [15–18]. In addition, these aromatic compounds have found their application in everyday foods [19]. The antimicrobial profile of coumarin derivatives has uncovered their inhibitory properties for the protease [20,21].

The demand of methods for the synthesis of structurally different coumarin derivatives have increased rapidly in response to the requirements in pharmaceutical and medical industries as new antibiotics [22]. For example, a series of 7-aminocoumarin derivatives with the heteroaryl moiety at C-3 position reported cytotoxic against the human umbilical vein endothelial cell line (HUVEC) and several other cancer cell lines [23]. Therefore, the idea was to study the antimicrobial activity of peptidomimetics containing the 7-aminocoumarin derivative can be toxic for model *E. coli* bacterial cell lines of K12, R2–R4 strains having different lipopolysaccharide lengths [22–33]. Thus, in this study, we used the synthetic potential of Ugi MCR to synthesize peptidomimetics and studied the influence of 7-aminocoumarins on bacterial cell lines. Moreover, coumarin derivatives were used as fluorescent sensors for estimation of the pH changes, as well as hydrogen peroxide detectors [34]. Overall, we expect that the synthesized peptidomimetics with 7-aminocoumarin scaffolds may strongly affect the bacterial membranes and the LPS included in them.

2. Materials and Methods

Commercially available reagents were ordered from Sigma-Aldrich and used without additional purification. The water and hexanes mixtures were prior distilled. Other solvents (analytical grade) were used without extra drying and purification. Solvents and volatile reagents were evaporated under reduced pressure. Reactions were performed in dry glass vessel under ambient conditions. Merck silica gel plates 60 F254 were applied for TLC (Thin Layer Chromatography) analysis. Crude mixture, after solvent evaporation, were purified by column chromatography on Merck silica gel 60/230–400 mesh, using an appropriate mixture of hexane and ethyl acetate as solvent. ^1H - and ^{13}C NMR (Nuclear Magnetic Resonance) spectra were recorded in Chloroform-*d* at Bruker 400 and Varian 500 MHz spectrometer using TMS (Trimethyl Silane) as an internal standard. Chemical shifts were reported in parts per million (ppm) and referred to residual deuterated solvent signal; coupling constants (*J*) were noted in Hz. High-resolution mass spectra (HR-MS) were recorded on the Maldi SYNAPT G2-S HDMS (Waters) apparatus with a QqTOF analyzer.

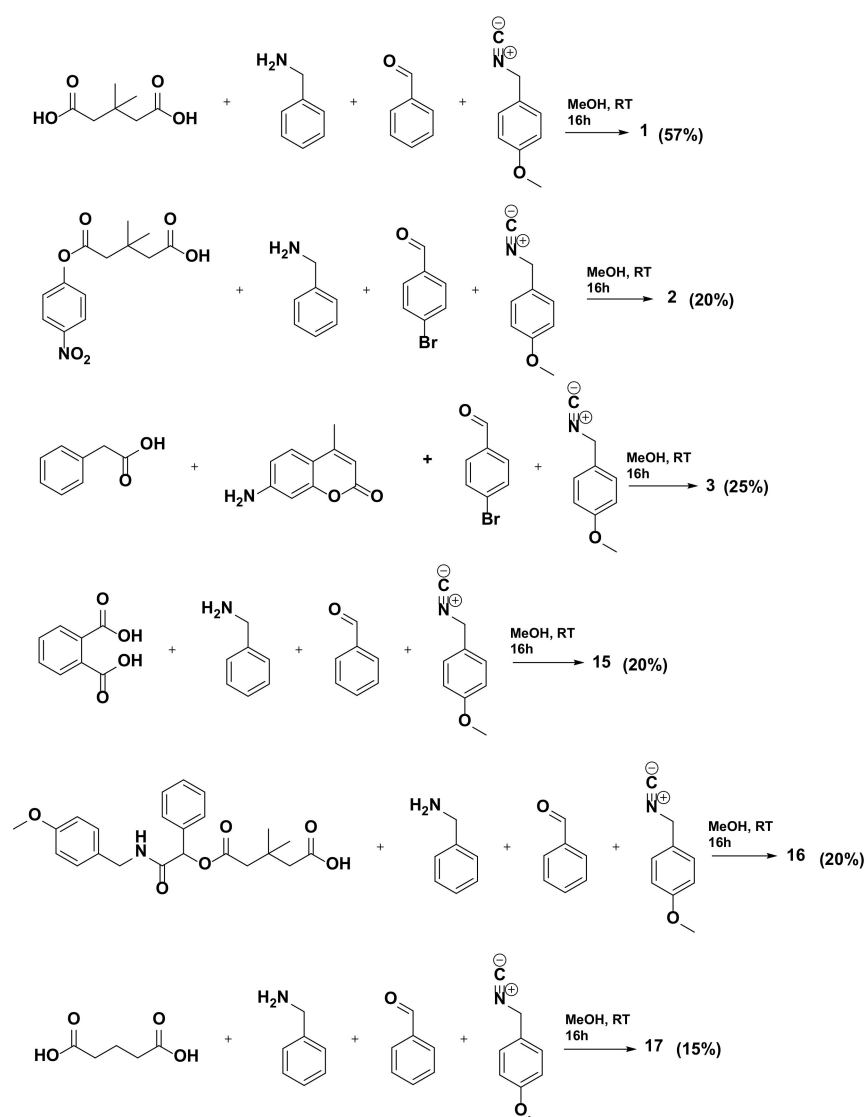
3. Experimental Section

3.1. Synthesis of *p*-Nitrophenylhydroxylglutarate

To the mixture of glutaric anhydride (1 g, 8.76 mmol) and *p*-nitrophenol (1.16 g, 8.94 mmol) in dichloromethane (10 mL), pyridine (5.5 mL) and 4-(dimethylamino)pyridine (5 mg) were added. The reaction mixture was stirred at 40 °C for 16 h. After that time, the solvent was evaporated. The residue was dissolved in ethyl ether (15 mL) and washed with 1 M hydrochloric acid (HCl), saturated copper sulfate (CuSO_4), and 5% sodium bicarbonate (NaHCO_3) in a respective manner. The extract was acidified with 35% HCl and extracted with ethyl acetate. The organic layer was dried on magnesium sulfate. The solvent was evaporated under vacuum, and the product was purified by column chromatography (silica gel, hexanes/ethyl acetate/acetic acid) to give light yellow solid (0.78 mg, 3.07 mmol). ^1H NMR (400 MHz, CDCl_3) δ 8.27 (d, *J* = 9.0 Hz, 1H), 7.28 (d, *J* = 9.0 Hz, 1H), 2.72 (t, *J* = 7.3 Hz, 1H), 2.54 (t, *J* = 7.1 Hz, 1H), 2.15–2.04 (m, 1H); ^{13}C NMR (101 MHz, CDCl_3) δ 178.4, 170.4, 155.3, 125.2, 122.4, 33.2, 32.6, 19.5. NMRs are in accordance with the earlier literature reports [34–56].

3.2. General Procedure for Synthesis of Compounds 1–17

To the solution of corresponding amine (1eq) in methanol (1 mL), respective aldehyde (1eq) was added and stirred at room temperature, for 30 min, followed by addition of carboxylic acid (1eq), and then we stirred the mixture for another 15 min. Then *p*-methoxybenzylisocyanide (1eq) added to the reaction mixture and stirred overnight at room temperature. Then the solvent was evaporated off under reduced pressure, and column chromatography was performed to get pure compounds (Schemes 1 and 2).



Scheme 1. Synthesis of compounds depicted in Figure 1.

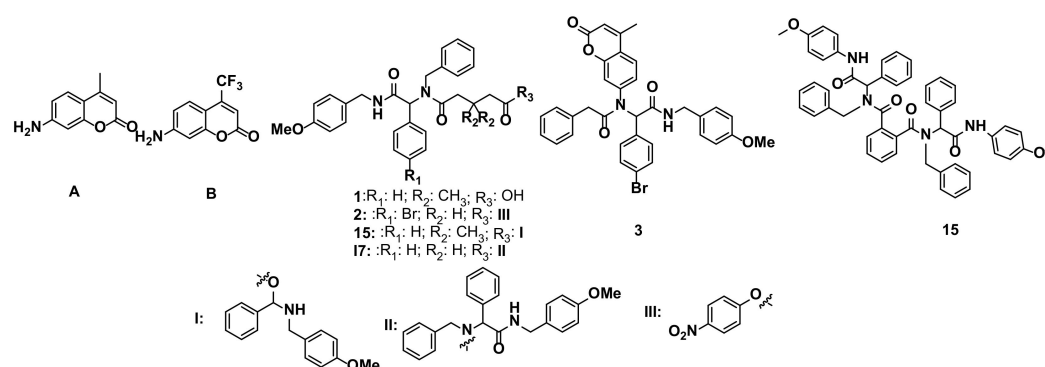
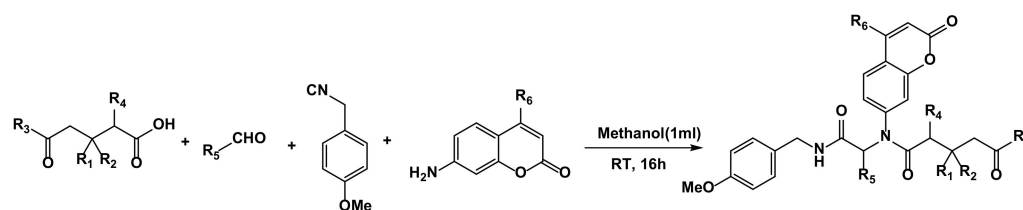


Figure 1. Structure of model compounds used in the studies.



Scheme 2. Synthesis of peptidomimetics 4–14.

3.2.1. (2-[(4-Methoxyphenyl)benzyl]amino-2-oxo-1-phenylethyl)-3,3-methyl-5-oxopentanoic acid (1)

Colorless oil (57%), $^1\text{H NMR}$ (400 MHz, CDCl_3) δ 7.30–7.09 (m, 11H), 6.89–6.77 (m, 4H), 6.06 (t, $J = 5.5$ Hz, 1H), 5.93 (s, 1H), 4.88 (d, $J = 17.6$ Hz, 1H), 4.56 (d, $J = 17.7$ Hz, 1H), 4.45–4.30 (m, 2H), 3.76 (s, 3H), 2.63–2.28 (m, 4H), 1.13 (d, $J = 38.1$ Hz, 6H). $^{13}\text{C NMR}$ (101 MHz, CDCl_3) δ 175.6, 169.0, 159.0, 136.4, 130.2, 128.9, 128.5, 126.0, 114.0, 63.9, 55.3, 43.3, 35.0, 29.4; HR-MS (ESI): m/z calculated for $\text{C}_{30}\text{H}_{34}\text{N}_2\text{O}_5$ $[\text{Na}]^+$ 525.5110, found 525.5109.

3.2.2. (2-[(4-Methoxyphenyl)-4-bromobenzyl]amino-2-oxo-1-phenylethyl)-5-(4-nitrophenoxy)-5-oxopentanoate (2)

Light brown oil. (25%) $^1\text{H NMR}$ (400 MHz, CDCl_3) δ 8.22 (d, $J = 9.2$ Hz, 2H), 7.34 (d, $J = 8.3$ Hz, 2H), 7.19 (d, $J = 9.2$ Hz, 8H), 7.01–6.92 (m, 2H), 6.82 (dd, $J = 8.7, 2.2$ Hz, 2H), 6.09 (s, 1H), 5.87 (s, 1H), 4.74 (d, $J = 17.7$ Hz, 1H), 4.56–4.25 (m, 3H), 3.77 (d, $J = 4.5$ Hz, 3H), 2.71–2.09 (m, 6H). $^{13}\text{C NMR}$ (126 MHz, CDCl_3) δ 173.8, 170.8, 168.9, 159.1, 155.4, 145.3, 137.0, 133.7, 131.2, 128.7, 127.3, 125.6, 123.0, 122.4, 114.1, 62.7, 55.3, 50.2, 43.3, 33.4, 32.6, 29.7, 20.1; HR-MS (ESI): m/z calculated for $\text{C}_{34}\text{H}_{32}\text{BrN}_3\text{O}_7$ $[\text{Na}]^+$: 697.4521, found 697.4528.

3.2.3. (2-[(4-Methoxyphenyl)-4-bromobenzyl]amino-5-[(4-methyl-2-oxo-2H-1-benzopyran-7-yl)amino]-phenylacetamide (3)

Yellow oil (46%). $^1\text{H NMR}$ (400 MHz, CDCl_3) δ 7.45–7.29 (m, 1H), 7.22 (d, $J = 8.3$ Hz, 2H), 7.21–7.12 (m, 5H), 7.08 (d, $J = 8.4$ Hz, 2H), 6.95 (d, $J = 8.5$ Hz, 4H), 6.76 (d, $J = 8.4$ Hz, 2H), 6.51 (s, 1H), 6.21 (s, 1H), 6.13 (s, 1H), 4.32 (d, $J = 5.6$ Hz, 2H), 3.72 (s, 3H), 3.39 (d, $J = 2.9$ Hz, 2H), 2.36 (s, 3H). $^{13}\text{C NMR}$ (101 MHz, CDCl_3) δ 171.3, 160.1, 158.1, 151.6, 142.4, 134.5, 133.0, 131.9, 131.7, 130.0, 129.0, 128.4, 126.9, 124.8, 123.0, 119.8, 115.8, 114.0, 64.1, 55.2, 43.2, 41.7, 18.6; *UV/Vis* (acetonitrile) $\lambda_{\text{max}} = 276$ nm; HR-MS (ESI): m/z calculated for $\text{C}_{34}\text{H}_{29}\text{BrN}_2\text{O}_5$ $[\text{Na}]^+$: 648.4200, found 648.4205.

3.2.4. (2-[(4-Methoxyphenyl)benzyl]amino-5-[(4-methyl-2-oxo-2H-1-benzopyran-7-yl)amino]-5-(4-nitrophenoxy)-5-oxopentanoate (4)

Colorless oil (55%). $^1\text{H NMR}$ (500 MHz, CDCl_3) δ 8.21 (s, 2H), 7.52 (s, 1H), 7.26–7.10 (m, 10H), 7.09 (s, 2H), 6.80 (s, 2H), 6.74 (s, 1H), 6.17 (s, 1H), 5.91 (s, 1H), 4.42 (s, 2H), 3.74 (s, 3H), 3.57 (s, 3H), 2.62 (s, 2H), 2.36–1.88 (m, 4H). $^{13}\text{C NMR}$ (126 MHz, CDCl_3) δ 172.0, 170.7, 169.2, 160.1, 159.0, 155.3, 153.3, 151.5, 145.2, 142.8, 133.7, 130.2, 129.8, 129.1, 128.5, 126.7, 125.1, 124.8, 122.4, 119.6, 119.2, 115.7, 114.0, 65.1, 55.3, 43.4, 33.7, 33.2, 20.2, 18.6; *UV/Vis* (acetonitrile) $\lambda_{\text{max}} = 275$ nm. HR-MS (ESI): m/z calculated for $\text{C}_{30}\text{H}_{34}\text{N}_2\text{O}_9$ $[\text{Na}]^+$: 686.2114, found 686.2117.

3.2.5. (2-[(4-Methoxyphenyl)benzyl]amino-5-[(4-methyl-2-oxo-2H-1-benzopyran-7-yl)amino]-5-oxopentanoic acid (5)

White solid (90%). Melting point: 176 °C; $^1\text{H NMR}$ (500 MHz, CDCl_3) δ 8.05 (d, $J = 9.1$ Hz, 1H), 7.35 (s, 1H), 7.08 (dt, $J = 14.7, 4.1$ Hz, 7H), 6.85 (d, $J = 9.1$ Hz, 1H), 6.73 (d, $J = 8.6$ Hz, 2H), 6.19 (d, $J = 0.9$ Hz, 1H), 6.02 (d, $J = 9.1$ Hz, 2H), 5.87 (s, 1H), 4.34 (d, $J = 5.7$ Hz, 2H), 3.74 (s, 3H), 3.69 (s, 3H), 2.28 (d, $J = 3.8$ Hz, 2H), 2.14–2.02 (m, 2H), 1.89–1.79 (m, 2H). $^{13}\text{C NMR}$ (126 MHz, CDCl_3) δ 177.1, 172.6, 169.4, 162.4, 160.3, 159.0, 153.3, 151.7, 142.7, 141.1, 133.6, 130.2, 129.7, 128.9, 128.7, 126.6, 126.1, 124.9, 119.7, 119.1, 115.5, 114.2, 65.4, 60.4, 55.3, 43.4, 33.8, 32.8, 30.3, 29.6, 22.7, 21.0, 20.2, 18.6, 14.1; *UV/Vis* (acetonitrile) $\lambda_{\text{max}} = 283$ nm. HR-MS (ESI): m/z calculated for $\text{C}_{31}\text{H}_{30}\text{N}_2\text{O}_7$ $[\text{Na}]^+$: 565.4987, found 565.4980.

3.2.6. [5-((2-((4-Methoxybenzyl)amino)-2-oxo-1-phenylethyl)(2-oxo-4-(trifluoromethyl)-2H-chromen-7-yl)amino)-3,3-dimethyl-5-oxopentanoic acid] (**6**)

Pale yellow powder (13%). Melting point: 184 °C; ^1H NMR (500 MHz, CDCl_3) δ 7.52 (s, 1H), 7.23–7.12 (m, 8H), 7.10–7.06 (m, 2H), 6.80 (d, $J = 8.7$ Hz, 2H), 6.77 (s, 1H), 6.16 (s, 1H), 6.11 (s, 1H), 4.42 (d, $J = 5.7$ Hz, 2H), 3.75 (s, 3H), 2.58 (d, $J = 13.3$ Hz, 1H), 2.41 (d, $J = 13.2$ Hz, 1H), 2.30–2.22 (m, 2H), 1.02 (d, $J = 20.2$ Hz, 6H); ^{13}C NMR (126 MHz, CDCl_3) δ 173.9, 173.0, 171.2, 168.7, 159.0, 158.1, 154.0, 143.7, 140.6, 133.1, 129.7, 129.2, 128.9, 125.5, 124.5, 122.3, 119.9, 119.2, 114.0, 113.3, 65.6, 60.4, 55.3, 45.9, 43.4, 34.4, 29.1, 21.0, 14.2; *UV/Vis* (acetonitrile) $\lambda_{\text{max}} = 283$ nm; HR-MS (ESI) calculated for $\text{C}_{33}\text{H}_{31}\text{N}_2\text{O}_7\text{F}_3[\text{Na}]^+$: 647.1981, found 647.1979.

3.2.7. [4-Nitrophenyl-5-((2-((4-methoxybenzyl)amino)-2-oxo-1-phenylethyl)(2-oxo-4-(trifluoromethyl)-2H-chromen-7-yl)amino)-5-oxopentanoate] (**7**)

Yellow solid (32%). Melting point: 101 °C; ^1H NMR (600 MHz, CDCl_3) δ 8.21 (s, 2H), 7.52 (s, 1H), 7.26–7.11 (m, 9H), 7.09 (s, 2H), 6.80 (s, 2H), 6.74 (s, 1H), 6.17 (s, 1H), 5.91 (s, 1H), 4.42 (s, 2H), 3.74 (s, 3H), 2.62 (s, 2H), 2.25 (d, $J = 52.8$ Hz, 2H), 2.03 (s, 2H); ^{13}C NMR (151 MHz, CDCl_3) δ 171.7, 170.7, 169.1, 159.0, 145.3, 44.1, 133.5, 130.2, 129.7, 128.9, 128.8, 122.4, 119.9, 114.0, 113.1, 64.9, 55.2, 43.4, 33.7, 33.1, 20.1; *UV/Vis* (acetonitrile) $\lambda_{\text{max}} = 275$ nm; HR-MS (ESI) calculated for $\text{C}_{37}\text{H}_{30}\text{N}_3\text{O}_9\text{F}_3[\text{Na}]^+$ is 740.1829, found 740.1832.

3.2.8. [5-((2-((4-Methoxybenzyl)amino)-2-oxo-1-phenylethyl)(2-oxo-4-(trifluoromethyl)-2H-chromen-7-yl)amino)-5-oxopentanoic acid] (**8**)

Pale yellow powder (25%). Melting point: 180 °C, ^1H NMR (500 MHz, CDCl_3) δ 7.52 (s, 1H), 7.14 (d, $J = 32.8$ Hz, 9H), 6.79 (s, 2H), 6.74 (s, 1H), 6.22–6.18 (m, 1H), 6.17 (s, 1H), 4.39 (s, 2H), 3.74 (s, 3H), 2.40 (s, 1H), 2.32 (s, 2H), 2.16 (s, 2H), 1.89 (s, 2H); ^{13}C NMR (126 MHz, CDCl_3) δ 177.9, 172.3, 169.3, 158.9, 144.0, 140.7, 133.5, 130.2, 129.7, 128.9, 128.8, 127.7, 125.4, 122.3, 120.1, 119.9, 116.6, 114.0, 113.1, 64.9, 55.2, 43.3, 33.9, 32.7, 20.1. *UV/Vis* (acetonitrile) $\lambda_{\text{max}} = 277$ nm; HR-MS (ESI) calculated for $\text{C}_{31}\text{H}_{27}\text{F}_3\text{N}_2\text{O}_7[\text{Na}]^+$: 619.1668, found 619.1652.

3.2.9. [5-((2-((4-Methoxybenzyl)amino)-2-oxo-1-phenylethyl)(2-oxo-4-(trifluoromethyl)-2H-chromen-7-yl)amino)-4,5-dioxopentanoic acid] (**9**)

Pale yellow solid (25%). Melting point: 149 °C; ^1H NMR (400 MHz, CDCl_3) δ 7.47 (dd, $J = 8.8, 1.9$ Hz, 1H), 7.25–7.18 (m, 3H), 7.17–7.06 (m, 5H), 6.81 (d, $J = 8.7$ Hz, 2H), 6.74 (s, 1H), 6.07 (s, 1H), 5.91 (t, $J = 5.6$ Hz, 1H), 4.43 (d, $J = 5.6$ Hz, 2H), 3.76 (s, 3H), 3.18–2.98 (m, 2H), 2.53 (t, $J = 6.3$ Hz, 2H). ^{13}C NMR (126 MHz, CDCl_3) δ 198.8, 173.3, 168.8, 166.3, 158.7, 158.4, 153.5, 142.3, 133.8, 131.2, 130.5, 129.1, 128.6, 127.4, 126.8, 124.6, 119.1, 114.0, 112.6, 64.3, 63.3, 55.5, 42.4, 35.3, 27.1. *UV/Vis* (acetonitrile) $\lambda_{\text{max}} = 276$ nm; HR-MS (ESI) calculated for $\text{C}_{31}\text{H}_{25}\text{N}_2\text{O}_8\text{F}_3[\text{Na}]^+$: 633.1461, found 633.1448.

3.2.10. [5-((2-((4-Methoxybenzyl)amino)-1-(4-methoxyphenyl)-2-oxoethyl)(2-oxo-4-(trifluoromethyl)-2H-chromen-7-yl)amino)-3,3-dimethyl-5-oxopentanoic acid] (**10**)

Pale yellow solid (10%). Melting point: 185 °C; ^1H NMR (400 MHz, CDCl_3) δ 7.52 (d, $J = 7.9$ Hz, 1H), 7.11 (d, $J = 8.6$ Hz, 2H), 6.99 (d, $J = 8.7$ Hz, 2H), 6.80–6.71 (m, 4H), 6.69–6.59 (m, 3H), 6.37–6.28 (m, 1H), 6.13 (s, 1H), 4.37 (d, $J = 5.7$ Hz, 2H), 3.72 (s, 3H), 3.67 (s, 3H), 2.60–2.51 (m, 1H), 2.38 (d, $J = 13.6$ Hz, 1H), 2.23 (d, $J = 5.3$ Hz, 2H), 1.00 (d, $J = 15.2$ Hz, 7H); ^{13}C NMR (126 MHz, CDCl_3) δ 172.9, 171.9, 168.0, 158.9, 158.0, 157.1, 153.0, 142.8, 139.5, 130.6, 128.7, 127.9, 123.9, 121.3, 118.9, 115.9, 113.0, 112.3, 64.1, 54.3, 52.4, 44.9, 42.3, 33.4, 28.1; *UV/Vis* (acetonitrile) $\lambda_{\text{max}} = 276$ nm; HR-MS (ESI) calculated for $\text{C}_{34}\text{H}_{33}\text{N}_2\text{O}_8\text{F}_3[\text{Na}]^+$: 677.2087, found 677.2081.

3.2.11. [5-((2-((4-Methoxybenzyl)amino)-1-(4-nitrophenyl)-2-oxoethyl)(2-oxo-4-(trifluoromethyl)-2H-chromen-7-yl)amino)-3,3-dimethyl-5-oxopentanoic acid] (**11**)

Bright yellow powder (16%). Melting point: 191 °C; ^1H NMR (600 MHz, CDCl_3) δ 8.05–7.96 (m, 2H), 7.56 (d, $J = 8.4$ Hz, 1H), 7.41–7.35 (m, 2H), 7.20–7.13 (m, 3H), 6.86–6.75 (m, 4H),

6.57 (s, 1H), 6.23 (s, 1H), 4.46–4.39 (m, 2H), 3.76 (s, 3H), 2.56–2.40 (m, 3H), 2.30–2.14 (m, 2H), 1.03 (s, 6H). ^{13}C NMR (126MHz, CDCl_3) δ 175.1, 172.7, 167.9, 159.2, 157.8, 154.2, 147.9, 143.4, 140.6, 131.2, 129.4, 127.9, 127.0, 125.9, 123.7, 119.5, 117.1, 114.1, 113.7, 64.4, 55.3, 44.8, 43.6, 34.1, 29.0; *UV/Vis* (acetonitrile) $\lambda_{\text{max}} = 276$ nm; HR-MS (ESI) calculated for $\text{C}_{33}\text{H}_{30}\text{N}_3\text{O}_9\text{F}_3$ $[\text{Na}]^+$ 692.1832, found 692.1814.

3.2.12. [5-((1-((4-Methoxybenzyl)amino)-4-methyl-1-oxopentan-2-yl)(2-oxo-4-(trifluoromethyl)-2H-chromen-7-yl)amino)-3,3-dimethyl-5-oxopentanoic acid] (**12**)

Pale yellow oil (3%); ^1H NMR (200 MHz, CDCl_3) δ 7.45–7.31 (m, 2H), 7.21–7.12 (m, 5H), 7.12–7.02 (m, 5H), 7.03–6.96 (m, 3H), 6.84 (dd, $J = 40.4, 8.1$ Hz, 2H), 6.76–6.66 (m, 2H), 6.07 (s, 1H), 5.99 (t, $J = 5.8$ Hz, 1H), 5.86 (s, 1H), 4.35–4.23 (m, 4H), 3.68 (s, 3H), 2.71–2.19 (m, 6H). ^{13}C NMR (126MHz, CDCl_3) δ 177.2, 176.3, 172.8, 169.7, 159.1, 158.1, 154.4, 142.9, 140.7, 130.1, 129.4, 126.6, 126.0, 122.4, 120.2, 118.9, 116.9, 114.1, 113.7, 57.0, 55.3, 53.4, 44.8, 44.6, 43.4, 43.2, 37.7, 33.7, 32.3, 28.7, 27.9, 24.9, 22.6, 22.4; *UV/Vis* (acetonitrile) $\lambda_{\text{max}} = 277$ nm; HR-MS (ESI) calculated for $\text{C}_{31}\text{H}_{35}\text{N}_2\text{O}_7\text{F}_3$ $[\text{Na}]^+$: 627.2294 found 627.2290.

3.2.13. [5-((2-((4-Methoxybenzyl)amino)-2-oxo-1-(p-tolyl)ethyl)(2-oxo-4-(trifluoromethyl)-2H-chromen-7-yl)amino)-3,3-dimethyl-5-oxopentanoic acid] (**13**)

Pale yellow powder (20%). Melting point: 179 °C; ^1H NMR (400 MHz, CDCl_3) δ 7.54 (d, $J = 8.4$ Hz, 1H), 7.15–7.10 (m, 2H), 6.96 (s, 4H), 6.83–6.73 (m, 4H), 6.12 (s, 1H), 6.08 (d, $J = 7.1$ Hz, 1H), 4.40 (d, $J = 5.7$ Hz, 2H), 3.75 (s, 3H), 2.57 (m, $J = 13.4$ Hz, 4H), 2.40 (d, $J = 13.4$ Hz, 1H), 2.25 (d, $J = 4.3$ Hz, 2H), 2.22 (s, 3H), 1.01 (d, $J = 15.8$ Hz, 6H). ^{13}C NMR (126MHz, CDCl_3) δ 174.2, 172.8, 168.9, 159.0, 158.1, 154.0, 143.9, 139.1, 130.1, 129.7, 128.9, 127.6, 125.4, 119.9, 116.7, 114.0, 113.2, 65.4, 55.2, 45.8, 43.4, 34.3, 29.0, 21.1; *UV/Vis* (acetonitrile) $\lambda_{\text{max}} = 276$ nm; HRMS calculated for $\text{C}_{34}\text{H}_{33}\text{N}_2\text{O}_7\text{F}_3$ $[\text{Na}]^+$: 661.2138, found 661.2136.

3.2.14. [(E)-5-((1-((4-Methoxybenzyl)amino)-1-oxo-4-phenylbut-3-en-2-yl)(2-oxo-4-(trifluoromethyl)-2H-chromen-7-yl)amino)-3,3-dimethyl-5-oxopentanoic acid] (**14**)

Red-yellow solid (15%). Melting point 196 °C; ^1H NMR (400 MHz, CDCl_3) δ 7.74 (dt, $J = 8.6, 1.9$ Hz, 1H), 7.43 (d, $J = 2.0$ Hz, 1H), 7.36 (dd, $J = 8.6, 2.1$ Hz, 1H), 7.25 (d, $J = 1.9$ Hz, 5H), 7.23–7.20 (m, 2H), 6.86–6.79 (m, 4H), 6.63 (d, $J = 15.9$ Hz, 1H), 6.54 (t, $J = 5.9$ Hz, 1H), 6.28 (dd, $J = 15.9, 9.1$ Hz, 1H), 5.22 (d, $J = 9.1$ Hz, 1H), 4.48–4.36 (m, 2H), 3.76 (s, 3H), 2.45 (d, $J = 1.6$ Hz, 2H), 2.33–2.21 (m, 2H), 1.02 (d, $J = 6.2$ Hz, 6H). ^{13}C NMR (126MHz, CDCl_3) δ 174.2, 172.6, 168.4, 159.1, 157.9, 154.6, 144.9, 140.9, 138.4, 135.1, 129.8, 129.0, 128.8, 126.9, 126.3; *UV/Vis* (acetonitrile) $\lambda_{\text{max}} = 260$ nm; HR-MS (ESI) calculated for $\text{C}_{35}\text{H}_{33}\text{N}_2\text{O}_7\text{F}_3$ $[\text{Na}]^+$: 673.2138, found 673.2135.

3.2.15. N1,N2-Dibenzyl-N1,N2-bis(2-((4-methoxybenzyl)amino)-2-oxo-1-phenylethyl)phthalamide (**15**)

Colorless Oil (20%); ^1H NMR (400 MHz, CDCl_3) δ 8.12–7.99 (m, 2H), 7.80–7.65 (m, 4H), 7.41–7.15 (m, 24H), 6.93–6.86 (m, 4H), 5.84–5.77 (m, 2H), 4.66–4.50 (m, 8H), 3.87–3.73 (s, 6H). ^{13}C NMR (126 MHz, CDCl_3) δ 171.91, 168.09, 159.62, 137.47, 134.58, 133.43, 130.45, 130.42, 129.17, 129.02, 128.68, 128.48, 128.28, 127.74, 127.39, 126.49, 113.83, 64.29, 56.04, 48.97, 43.75. HR-MS(ESI) calculated for $\text{C}_{54}\text{H}_{50}\text{N}_4\text{O}_6$ $[\text{M}+\text{Na}]^+$: 873.3623, found 873.3628

3.2.16. {2-((4-Methoxybenzyl)amino)-2-oxo-1-phenylethyl-5-(benzyl(2-((4-methoxybenzyl)amino)-2-oxo-1-phenylethyl)amino)-3,3-dimethyl-5-oxopentanoate} (**16**)

White powder (20%). Melting point: 127 °C; ^1H NMR (600 MHz, CDCl_3) δ 8.04 (dd, $J = 8.2, 1.4$ Hz, 2H), 8.02–7.98 (m, 4H), 7.52–7.46 (m, 6H), 7.39 (t, $J = 7.8$ Hz, 5H), 7.33 (s, 2H), 7.19 (s, 3H), 7.09 (d, $J = 8.6$ Hz, 4H), 6.77 (d, $J = 8.6$ Hz, 4H), 6.30 (d, $J = 6.3$ Hz, 4H), 4.41 (dd, $J = 14.7, 5.9$ Hz, 2H), 4.35 (s, 1H), 3.72 (s, 6H), 2.10 (s, 2H), 1.36 (s, 1H), 1.19 (s, 6H). ^{13}C NMR (151 MHz, CDCl_3) δ 168.2, 164.9, 159.1, 135.5, 133.6, 133.6, 130.2, 129.8, 129.8, 129.2, 129.0, 128.9, 128.8, 128.6, 128.5, 127.3, 114.1, 75.9, 55.3, 42.9, 29.7; HR-MS (ESI) calculated for $\text{C}_{51}\text{H}_{52}\text{N}_4\text{O}_6$ $[\text{Na}]^+$: 778.3492, found 778.3496.

3.2.17. {N1,N5-Dibenzyl-N1,N5-bis(2-((4-methoxybenzyl)amino)-2-oxo-1-phenylethyl)glutaramide} (17)

White powder (20%). Melting point: 147 °C; ¹H NMR (400 MHz, CDCl₃) δ 7.49–7.44 (m, 4H), 7.40–7.30 (m, 10H), 7.29–7.25 (m, 8H), 7.19–7.13 (m, 6H), 7.06 (dd, *J* = 7.5, 2.1 Hz, 2H), 6.85–6.80 (m, 2H), 6.00 (s, 2H), 5.50 (s, 2H), 4.75 (d, *J* = 16.5 Hz, 1H), 4.54–4.31 (m, 3H), 3.78 (s, 6H), 1.43 (s, 1H), 1.26 (s, 4H), 0.88 (s, 1H). ¹³C NMR (126 MHz, CDCl₃) δ 174.6, 169.5, 158.9, 137.3, 135.1, 130.3, 129.9, 128.8, 128.6, 128.5, 128.3, 126.9, 126.2, 113.9, 63.4, 55.2, 43.1, 32.5; HR-MS (ESI) calculated for C₅₁H₅₂N₄O₆ [Na]⁺: 839.3785, found 839.3765.

4. Microorganisms and Media

All microbial experiments were described in detail in References [22,34,47–54].

The compounds described in our earlier works, such as coumarin derivatives, new ionic liquids based on theophylline, quaternary ammonium ionic liquids, 1,2-diarylethanol derivatives, α-amidoamides, and lactones, were tested for their cytotoxic activity against model Gram-negative bacteria in model *Escherichia coli* K12 (without LPS in its structure) and R2–R4 (with different LPS length in its structure), (Collection of strains of Ludwik Hirszfeld Institute of Immunology and Experimental Therapy-Polish Academy of Sciences), strains as new potential candidates for antibacterial drugs. All analyzed compounds belong to the so-called A group of peptidomimetics. These are compounds whose structure and function are similar to those of peptides. They constitute an important group of compounds with biological, microbiological, anti-inflammatory, and anticancer properties. Therefore, research on new peptidomimetics that burden the action of native peptides, the half-life of which in the body is much longer due to structural modifications, is extremely important [1–55]. In addition, in the presented studies, based on the conducted minimum inhibitory concentration (MIC) and minimum inhibitory concentration (MBC) tests, it was shown that the antibacterial (toxic) activity of the analyzed peptidomimetics strictly depends on their structure and the type of a specific substituent, which may be an amino, hydroxyl, carboxylic group, aromatic ring, esters, or an aliphatic chain. These compounds affect the bacterial structure of the cell wall of various lengths and the LPS contained therein in the membrane of the model strains analyzed, especially in the region of the O antigen, the outermost layer of the LPS. In addition, the isolation of bacterial DNA and the study of its oxidative damage were performed after modification with the analyzed compounds after the use of specific enzymes from the group of repair glycosylases, which includes the Fpg protein (Labjot, New England Biolabs, UK). The analyzed damage values after digestion with the Fpg protein were compared to the modification with the corresponding antibiotics, such as kanamycin, streptomycin, ciprofloxacin, bleomycin, and cloxacillin [56–59]. The presented research clearly shows that the analyzed derivative peptidomimetics can be used as new potential “candidates” for new drugs in relation to commonly used drugs, such as the analyzed antibiotics. Their chemical and biological activity is related to the aromatic and aliphatic groups in the structure of the substituent, for example. The observed results are especially important in the case of growing bacterial resistance to various drugs and antibiotics, especially in nosocomial infections and neoplasms, and in the era of pandemics caused by microorganisms. The distribution of the basic types of oligosaccharides in *Escherichia coli* lipopolysaccharides and the lipopolysaccharide-associated common enterobacterial antigen (ECA LPS) found in rough *Escherichia coli* R1, R2, and R4 strains is an ideal model for assessing the efficacy of Basic Antibiotic Parameters. Based on our own research of the analyzed compounds cited in References [47–51], we rely on their characteristics described in References [52–54].

5. Results and Discussion

5.1. Chemistry

For our research, to synthesize a series of peptidomimetics, we used 7-amino-4-methylcoumarin (**A**) and 7-amino-4-(trifluoromethyl)coumarin (**B**) as amines. For comparison, we synthesized compounds without coumarin, using 3,3-dimethylglutaric acid,

a benzylamine, a benzaldehyde, and *p*-methoxybenzylisocyanide with 57% yield. Then the Ugi-reaction product **1** was used as an acid in the following Passerini reaction with benzaldehyde, benzylamine, and a *p*-methoxybenzyl isocyanide to give the product **16** with 20% yield. The product **17** was formed in the double-Ugi reaction proceeding along with glutaric acid, benzylamine, benzaldehyde, and a *p*-methoxybenzyl isocyanide (20% yield). Then we replaced the glutaric acid to phthalic acid by keeping other components same as in **17**, to get compound **15** (20% yield). Product **2** was obtained in the Ugi reaction, using *p*-nitrophenylhydrogenlutarate, *p*-bromobenzylamine, benzaldehyde, and *p*-methoxybenzyl isocyanide (25%). Further the glutaric acid was exchanged with phenylacetic acid for peptidomimetic **3** with benzylamine, *p*-bromobenzaldehyde, and *p*-methoxybenzylisocyanide (25% yield). The compounds were synthesized as shown in Scheme 1, and the structures are represented in Figure 1.

The structures of synthesized peptidomimetics are depicted in Figures 2 and 3. In Scheme 1, we have mentioned about the model peptidomimetics (**1–3** and **15–17**) synthesized for highlighting the effect of each component of Ugi reaction in studied antimicrobial activities.

While Scheme 2 shows the library of peptidomimetics (4–14) containing aminocoumarin scaffolds.

For product **4**, *p*-nitrophenol ester of glutaric acid was used, along with 7-amino-4-methylcoumarin, benzaldehyde, and *p*-methoxybenzylisocyanide, which gave corresponding peptidomimetic with 25% yield. When glutaric acid was put to the reaction mixture by keeping other components the same as in compound **4**, the peptidomimetic **5** was obtained with 90% yield. When we used the 7-amino-4-trifluoromethyl coumarin with 2,2-dimethylglutaric acid, benzaldehyde, and *p*-methoxybenzylisocyanide, it gave compound **6** with 13% yield. Then, for compound **7**, we took *p*-nitrophenol ester of glutaric acid, keeping other components the same as in **6** to get 32% yield of the corresponding peptidomimetic. For compound **9**, we used 2-ketoglutaric acid and kept the other component the same as in **6** and **7**, and we obtained the product with 25% yield. Then, to study the effect of aldehyde group on bioactivity, we synthesized compounds **8**, **10**, **11**, **12**, **13**, and **14** with 7-amino-4-trifluoromethylcoumarin, glutaric acid (2,2-dimethylglutaric acid for **8**), *p*-methoxybenzylisocyanide using benzaldehyde, *p*-methoxybenzaldehyde, *p*-nitrobenzaldehyde, isovaleric aldehyde, *p*-methylbenzaldehyde, and cinnamaldehyde respectively to obtain peptidomimetics with yields mentioned in Table 1.

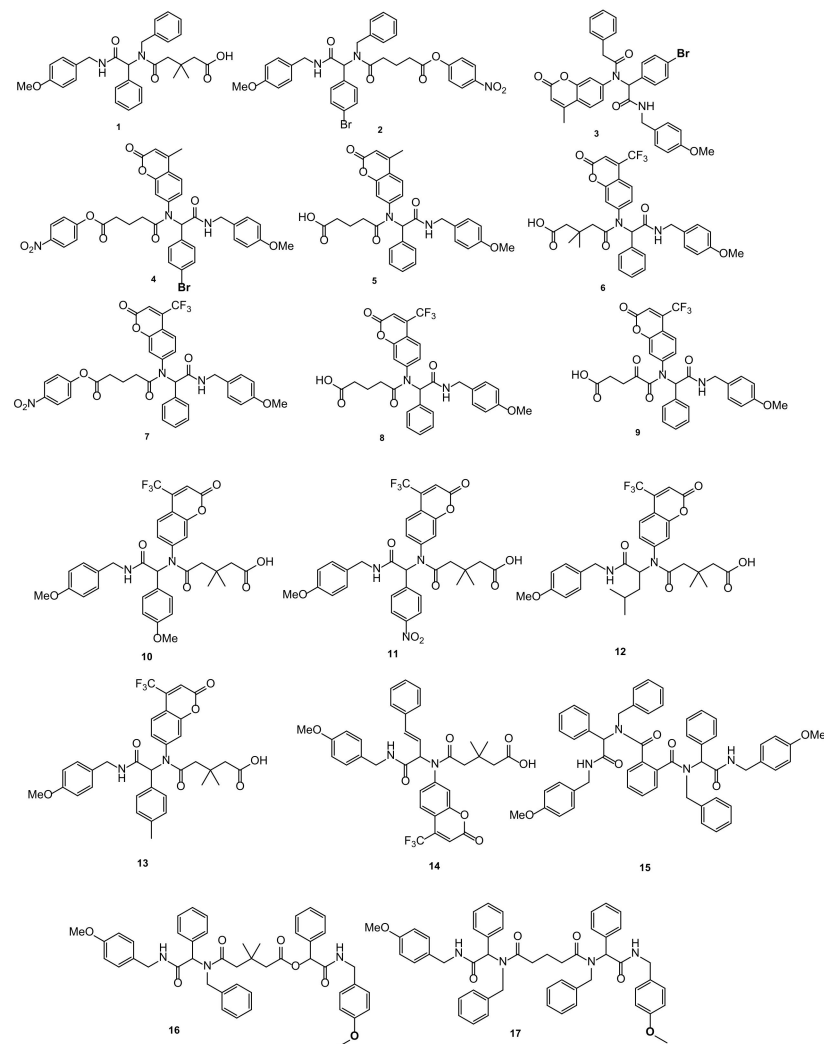


Figure 2. Structure of investigated peptidomimetics (in parentheses are given the corresponding numbering used during chemical syntheses).

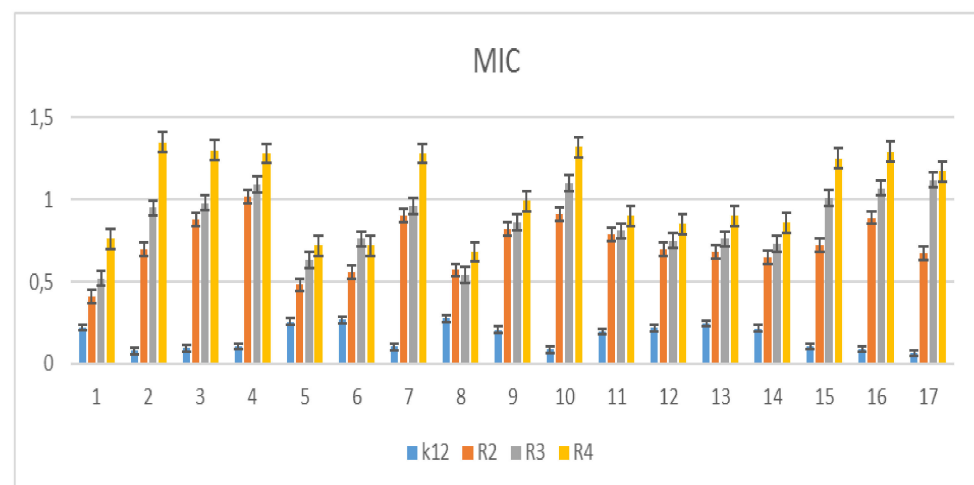


Figure 3. Minimum inhibitory concentration (MIC) of the coumarin derivatives in model bacterial strains. The *x*-axis features coumarin derivatives 1–17 used sequentially. The *y*-axis shows the MIC value in $\mu\text{g}/\text{mL}^{-1}$. Investigated strains of *E. coli* K12 as control (blue), R2 strains (orange), R3 strain (grey), and R4 strain (yellow). The *y*-axis shows the MBC value in $\mu\text{g}/\text{mL}^{-1}$. The order in which the compounds were applied to the plate are shown in Supplementary Materials Figure S1.

Table 1. Peptidomimetics synthesized by Scheme 2.

Entry	R ₁	R ₂	R ₃	R ₄	R ₅	R ₆	Product Symbol	Yield (%)
1	H	H	4-NO ₂ -C ₆ H ₄ OH	H	C ₆ H ₅	CH ₃	4	25
2	H	H	OH	H	C ₆ H ₅	CH ₃	5	90
3	H	H	4-NO ₂ -C ₆ H ₄ OH	H	C ₆ H ₅	CF ₃	7	32
4	CH ₃	CH ₃	OH	H	C ₆ H ₅	CF ₃	6	13
5	H	H	OH	H	C ₆ H ₅	CF ₃	8	25
6	CH ₃	CH ₃	OH	H	<i>p</i> -OCH ₃ -C ₆ H ₄	CF ₃	10	10
7	CH ₃	CH ₃	OH	H	<i>p</i> -NO ₂ -C ₆ H ₄	CF ₃	11	16
8	CH ₃	CH ₃	OH	H	CH ₂ CH(CH ₃) ₂	CF ₃	12	3
9	CH ₃	CH ₃	OH	H	<i>p</i> -CH ₃ -C ₆ H ₄	CF ₃	13	20
10	CH ₃	CH ₃	OH	H	CH=CH-C ₆ H ₅	CF ₃	14	25
11	O		OH	O	C ₆ H ₅	CF ₃	9	25

Reaction conditions: all components of Ugi reaction were used 0.25 mmol, in methanol (1 mL), for 24 h, at RT (room temperature), and purified by column chromatography.

5.2. Cytotoxic Studies of the Library of Peptidomimetics

In general, the obtained results depict that the 7-aminocoumarin scaffold present in the peptidomimetics has an inhibitory effect on each bacterial model studied. Interestingly, the presence of the ester group in compound 4 resulted in increased minimal inhibitory concentration compared to the similar structure with free carboxylic acid group (compound 5). The substituents, such as the (3,3)-dimethyl group introduced into carboxylic acid, have a slight impact on the activity of peptidomimetics (compounds 6 and 8). We observed that the changing of the aldehyde in the Ugi reaction also does not affect the activity of investigated peptidomimetics. Interestingly, the compounds containing 7-amino-4-(trifluoromethyl)-coumarin possess a high inhibitory effect compared to those containing 7-amino-4-methyl-coumarin (compounds 4 and 7). Unexpectedly, the peptidomimetics obtained by the Ugi–Passerini reaction (16) and the double-Ugi reaction (17) have shown high inhibitory activity despite relatively extensive structure.

The minimal inhibitory concentration (MIC) values for each model *E. coli* R2–R4 and K12 strains were visible on all analyzed microplates after the addition of the microbial growth index (resazurin). On the first plate, where the K12 strains were analyzed, the color change was observed already at a dilution of 10⁻³, and the MIC values of compounds shown in Table 2 were calculated at a concentration of 0.02 μM.

Table 2. Statistical analysis of all analyzed compounds by MIC, MBC, and MBC/MIC; <0.05 *, <0.01 **, <0.001 ***.

No. of Samples	2	3	4	7	10	15	16	17	Type of Test
K12	***	**	***	**	**	*	**	**	MIC
R2	***	**	***	**	**	*	***	**	MIC
R3	***	**	***	**	**	*	**	**	MIC
R4	***	**	***	**	**	*	**	**	MIC
K12	***	**	**	**	**	*	**	**	MBC
R2	**	**	**	**	**	*	**	**	MBC
R3	**	**	**	**	**	*	**	**	MBC
R4	**	**	**	**	**	*	**	**	MBC
K12	*	**	*	*	*	*	**	*	MBC/MIC
R2	*	*	*	*	*	*	**	*	MBC/MIC
R3	*	*	*	*	*	*	**	*	MBC/MIC
R4	*	*	*	*	*	*	**	*	MBC/MIC

On the second plate, where strain R2 was present, the color change was observed already at the dilution of 10⁻⁴, and the MIC value of compounds shown in Table 2 were calculated at a concentration of 0.002 μM for the abovementioned compounds 2, 3, 4, 7,

10, 15, 16, and 17. On the third plate, where the R3 strain was used, the color change for the analyzed compounds was already at a dilution of 10⁻², corresponding MIC values were calculated for the compounds shown in Table 2, at a concentration of 0.005 μM . On the fourth plate, where the R4 strain was analyzed, a color change was observed for the analyzed compounds already at a dilution of 10⁻², which corresponds to the MIC values of compounds shown in Table 2 were calculated at a concentration of 0.02 μM . Similar values were observed for the minimal bactericidal concentration (MBC) test (see Supplementary Materials). Increasing MBC values were observed for all 17 compounds analyzed. Bacterial strains, R3, and R4, were more sensitive compared to k12 and R2 to the analyzed compounds in both types of MIC and MBC assays. Strain R4 was the most sensitive among all strains probably due to the longer length of the lipopolysaccharide chain. In all analyzed cases, the MBC values were approximately 20 times higher than the MIC values (Figure 4). Modification of functional groups in the analyzed aminocoumarin peptidomimetics probably changes the MBC/MIC ratio, and it strongly depends on the specific functional groups as a function of the substituent, which can be clearly observed from the obtained data for analyzed strains (Figures 3–6 and Table 1).

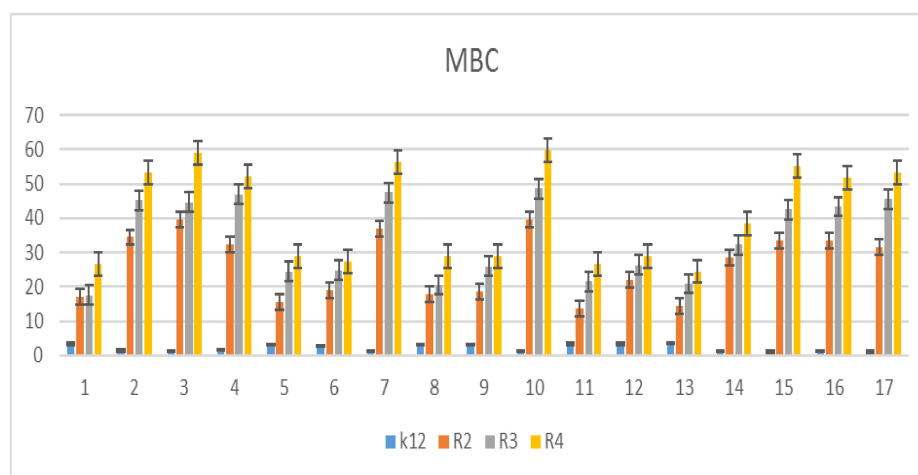


Figure 4. MBC of the coumarin derivatives in model bacterial strains. On the *x*-axis, 17 compounds were used sequentially. The *y*-axis shows the MBC value in $\mu\text{g}/\text{mL}^{-1}$ (see Supplementary Materials).

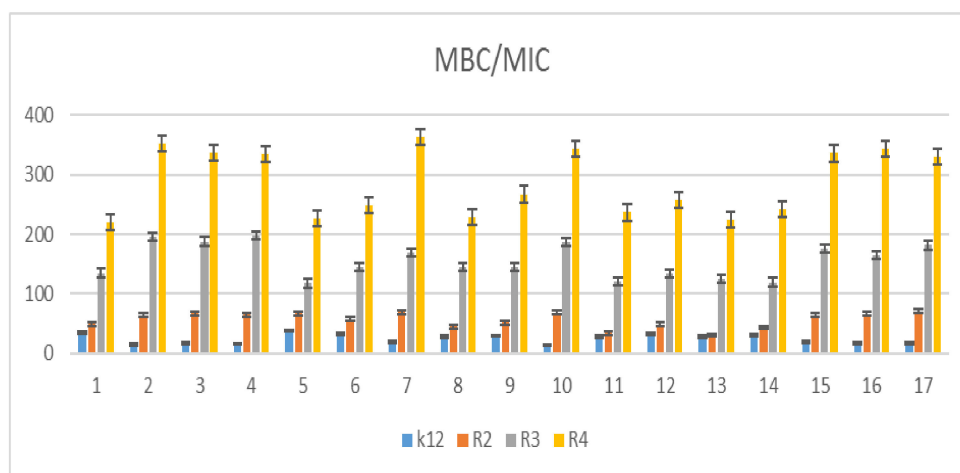


Figure 5. MBC/MIC of the coumarin derivatives in model bacterial strains. On the *x*-axis, compounds 1–17 are used sequentially. The *y*-axis shows the MBC/MIC value in $\mu\text{g}/\text{mL}^{-1}$ (see Supplementary Materials).

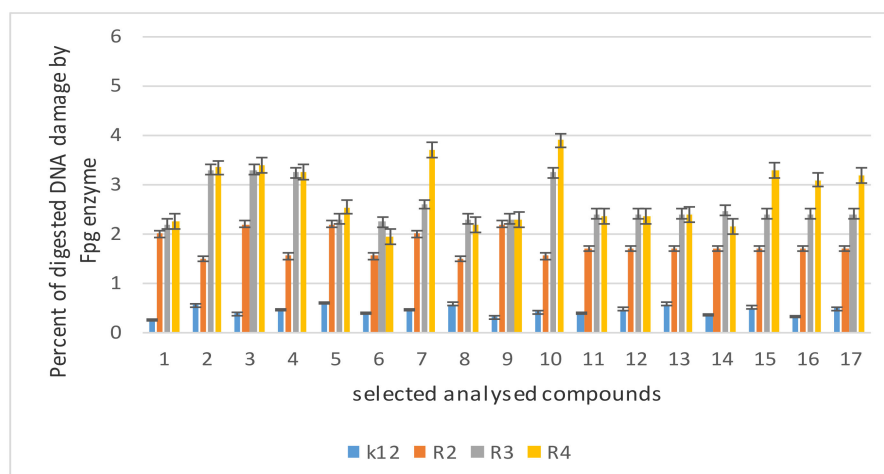


Figure 6. Percentage of plasmid DNA recognized by Fpg enzyme (*y*-axis) with model bacterial, K12, and R2–R4 strains (*x*-axis). The compounds numbered 2, 3, 4, 7, 10, 15, 16, and 17 were statistically significant at <0.05 *.

5.3. Modification of Bacterial DNA Isolated from *E. coli* R2–R4 Strains with Tested Coumarin Derivatives

The MIC values indicate that the toxicity of the tested compounds to the analyzed model bacterial strains K12 and R2–R4 should increase with the increase in the number of aromatic rings in peptidomimetics and the appropriate length of the alkyl chain. Among all peptidomimetics, the toxicity was particularly visible for compounds marked with numbers 2, 3, 4, 7, 10, 15, 16, and 17. As in our previous work, only on the basis of the MIC and MBC values, we selected compounds for further research. We wanted to observe the effect of modification of coumarin peptidomimetics on the isolated bacterial DNA after digestion with the Fpg protein, where the amount of damage should be particularly visible in the form of continuous bands. Moreover, for further DNA analyses, based on MIC values, we selected only two strains (K12, lacking the LPS chain; and R4, having the longest LPS chain). This interaction was observed especially for a specific length of the alkyl chain with an increasing number of aromatic rings.

The results of plasmid DNA modified by coumarin peptidomimetics (Figure 6 after Fpg treatment) showed that all analyzed peptidomimetics with different alkyl chain length and substituents containing a phenolic hydroxyl group or carboxylic acid group can strongly change the topological forms of plasmids, even after digestion with the Fpg protein.

In bacterial DNA isolated from all model strains modified with selected coumarin derivatives and digested by Fpg protein, a change in the main topological forms of the plasmid, ccc, oc, and linear was observed. Over 3% of oxidative damage was identified after digestion of Fpg, which may indicate that coumarin derivatives strongly damage plasmid DNA because of oxidative stress generated in the cell upon induction with the analyzed compounds, which causes oxidation of DNA base pairs and their modification as new substrates for Fpg protein in addition to 8-oxoguanine, commonly known from the literature. Moreover, the composition and length of lipopolysaccharide (LPS) may influence the toxicity of model target bacterial cell lines. Our observations indicate that the alkyl chain length of peptidomimetics can determine toxicity to certain *E. coli* R-strains, as evidenced by the MIC and MBC values [29–55].

The obtained results were also statistically significant at the level of $p < 0.05$. In the analyzed coumarin derivatives, especially for compounds 2, 3, 4, 7, 10, 15, 16, and 17, the MIC values were similar to those in the R4 model strain, which proves that these compounds can also potentially be used as “substitutes for” commonly used antibiotics—Figure 7.

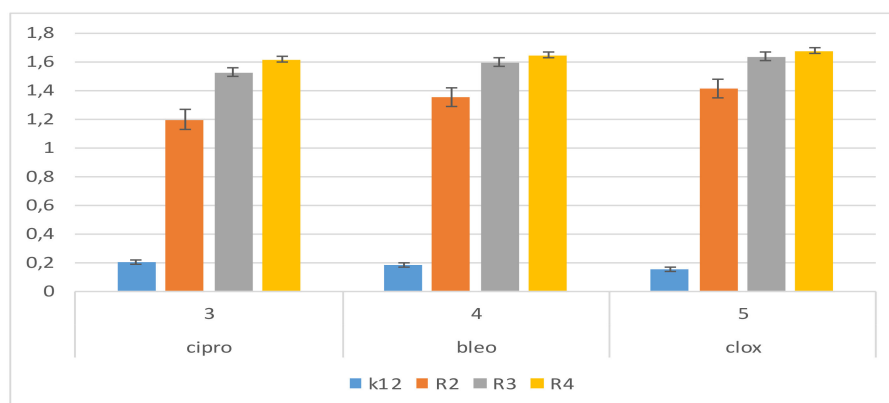


Figure 7. Examples of MIC with model bacterial strains K12, R2, R3, and R4 for studying antibiotics ciprofloxacin, bleomycin, and mechanism. The x -axis features antibiotics used sequentially. The y -axis features the MIC value in $\mu\text{g}/\text{mL}^{-1}$.

In the DNA obtained from model bacterial strains after modifications with antibiotics and digestion with Fpg protein, no significant changes were observed in all topological forms in different proportions (Supplementary Materials Figure S3). This proves that modifications with antibiotics are less absorbed by the Fpg protein than the modifications of coumarin peptidomimetics on bacterial DNA (Figure 8). This may indicate that modification with an appropriate antibiotic in bacterial DNA does not produce new compounds for the bacterial glycosylase.

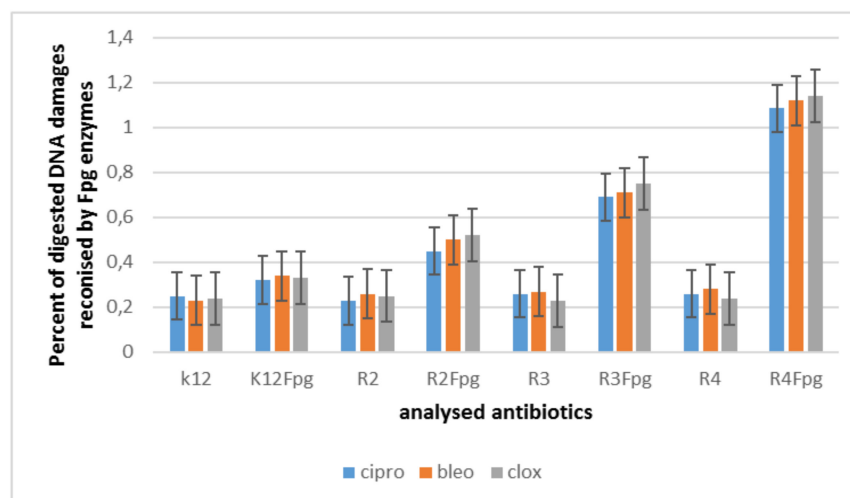


Figure 8. Percentage of bacterial DNA recognized by Fpg enzyme in model bacterial strains after ciprofloxacin, bleomycin, and cloxacillin treatment. The compounds were statistically significant at $p < 0.05$.

The highest damage in plasmid DNA was observed for compounds numbered as 2, 3, 4, 7, 10, 15, 16, and 17. The samples modified with three different antibiotics were lower and not as clear as for the analyzed coumarin derivatives. The reactivity of *E. coli* strains after modification with coumarin derivatives and digestion with Fpg protein was as follows: $R4 > R2 > R3 > K12$, and this effect was very similar to our previous research [35,36,43–51]. This indicates a very high toxicity of the analyzed coumarin peptidomimetics on bacterial DNA through a significant modification of the components of the bacterial membrane and the LPS contained in it, which may activate bacterial topoisomerases, or may affect the relaxation of the structure and access to modified, exposed DNA bases.

Stabilization of the topoisomerase-controlling complex is presumably necessary for cell survival. Blocking these enzymes blocks replication and transcription, which can affect the total amount of super replicated DNA.

6. Conclusions

Considering the importance of coumarin derivatives, we synthesized the diverse peptidomimetics containing the 7-amino-4-methylcoumarin and 7-amino-4-(trifluoromethyl)coumarin via the Ugi four-component reaction and evaluated them as new potential antimicrobial drugs against various types of Gram-stained bacteria by lipopolysaccharide (LPS). We focused on the role of aldehydes and carboxylic acids used in the Ugi reaction on the biological activities of peptidomimetics possessing the 7-aminocoumarin scaffold. The obtained results revealed the strong influence of the carboxylic acid group on the MIC values for various *E. coli* strains R2–R4 and K12. These compounds present the important group. Moreover, we compared the activity demonstrated by the peptidomimetics containing benzylamine instead of 7-aminocoumarin, which is in line with our research hypothesis. The abovementioned results are important for research on the mechanism of toxic action of new drugs (peptidomimetics) based on coumarin derivatives, which can damage the bacterial cell membrane by changing its surface charge, and it may play an important role in reducing antibiotic resistance, with a particular effect observed for compounds 2, 3, 4, 7, 10, 15, 16, and 17, which showed defined MIC values and MBC/MIC ratios. Compounds nos. 7 and 14 showed super-selectivity in all analyzed bacterial strains. The reported compounds can be specific for *E. Coli*; to find the core of mechanistic action for the interaction of peptidomimetics and *E. Coli*, we will study deeply in our ongoing research. The presented studies concern only model *E. coli* bacterial septic hats. In the future, cytotoxicity studies will also be performed by using different cell lines and cultures to assess the biocompatibility of test compounds and also to address the DRESS syndromes [57] for the active peptidomimetics.

Supplementary Materials: The following are available online at <https://www.mdpi.com/article/10.3390/ma14195725/s1>. Figure S1: Examples of MIC and MBC on microplates with different concentration of studied compounds (mg L^{-1}). Figure S2: Example of an agarose gel electrophoresis separation of isolated plasmids DNA from R4 strains modified with selected coumarin derivatives. Figure S3: Example of an agarose gel electrophoresis separation of isolated plasmids DNA from R4 strains modified with antibiotics: cloxacillin, ciprofloxacin, and bleomycin digested (or not) with repair enzymes Fpg.

Author Contributions: Conceptualisation or design of the work, P.K. (Paweł Kowalczyk) and R.O.; methodology, P.K. (Paweł Kowalczyk), M.W., P.P., R.O., M.S., K.K., S.R., G.S., D.S. and P.K. (Patrycja Kleczkowska); synthesis of all compounds, M.W., R.O. and P.P.; software, P.K. (Paweł Kowalczyk) and M.S.; validation, P.K. (Paweł Kowalczyk), M.W., P.P., R.O., M.S., K.K., S.R., G.S., D.S. and P.K. (Patrycja Kleczkowska); formal analysis, P.K. (Paweł Kowalczyk) M.W., P.P. and R.O.; investigation, P.K. (Paweł Kowalczyk), M.S., D.S. and P.K. (Patrycja Kleczkowska); interpretation of data for the work, P.K. (Paweł Kowalczyk) and R.O.; drafting the work, P.K. (Paweł Kowalczyk) and R.O.; revising it critically for important intellectual content; P.K. (Paweł Kowalczyk), R.O. and K.K. resources; P.K. (Paweł Kowalczyk), R.O., K.K., D.S. and P.K. (Patrycja Kleczkowska); data curation, P.K. (Paweł Kowalczyk) and R.O.; writing of the original draft preparation, P.K. (Paweł Kowalczyk) and R.O.; writing of review and editing, P.K. (Paweł Kowalczyk); visualization, P.K. (Paweł Kowalczyk) and M.S.; supervision, P.K. (Paweł Kowalczyk) and R.O.; project administration, P.K. (Paweł Kowalczyk) and R.O.; funding acquisition, K.K. All authors have read and agreed to the published version of the manuscript.

Funding: This work was supported by a grant from the Medical University of Białystok SUB/2DN/21/001/2201 and by the National Science Center, Poland, project OPUS No. 2019/33/B/ST4/01118.

Institutional Review Board Statement: Not applicable.

Informed Consent Statement: Not applicable.

Data Availability Statement: Upon request of those interested.

Acknowledgments: The authors thank Jolanta Łukasiewicz from Ludwik Hirszfeld Institute of Immunology and Experimental Therapy (Polish Academy of Sciences) for providing the strains of *E. coli*. We would also like to thank Dominik Koszelewski for his contribution to the analysis of the obtained data.

Conflicts of Interest: The authors declare no conflict of interest.

Abbreviations

MIC	minimum inhibitory concentration
MBC	minimum bactericidal concentration
Oc	open circle
Ccc	covalently closed circle

References

1. Dömling, A.; Ugi, I. Multicomponent Reactions with Isocyanides. *Angew. Chem. Int. Ed.* **2000**, *39*, 3168–3210. [[CrossRef](#)]
2. Das, K.; Jain, B.; Gupta, P. Photophysics of Coumarin 500 and Coumarin 151 in AOT reverse micelles. *Chem. Phys. Lett.* **2005**, *410*, 160–164. [[CrossRef](#)]
3. Kumar, S.; Mukesh, K.; Harjai, K.; Singh, V. Synthesis of coumarin based Knoevenagel-Ugi adducts by a sequential one pot five-component reaction and their biological evaluation as anti-bacterial agents. *Tetrahedron Lett.* **2019**, *60*, 8–12. [[CrossRef](#)]
4. Marquarding, D.; Gokel, G.; Hoffmann, P.; Ugi, I. Chapter 7—The Passerini Reaction and Related Reactions. *Org. React.* **1971**, *20*, 133. [[CrossRef](#)]
5. Bos, M.; Riguet, E. Synthesis of Chiral γ -Lactones by One-Pot Sequential Enantioselective Organocatalytic Michael Addition of Boronic Acids and Diastereoselective Intramolecular Passerini Reaction. *J. Org. Chem.* **2014**, *79*, 10881–10889. [[CrossRef](#)]
6. Bossio, R.; Marcaccini, S.; Pepino, R.; Torroba, T. Synthesis Studies on Isocyanides and Related Compounds: A Novel Synthetic Route to Furan Derivatives. *Heterocycles* **1993**, *1983*, 783. [[CrossRef](#)]
7. Szymanski, W.; Ostaszewski, R. Toward stereocontrolled, chemoenzymatic synthesis of unnatural peptides. *Tetrahedron* **2008**, *64*, 3197–3203. [[CrossRef](#)]
8. Szymanski, W.; Zwolinska, M.; Ostaszewski, R. Studies on the application of the Passerini reaction and enzymatic procedures to the synthesis of tripeptide mimetics. *Tetrahedron* **2007**, *63*, 7647–7653. [[CrossRef](#)]
9. Szymanski, W.; Ostaszewski, R. Multicomponent diversity and enzymatic enantioselectivity as a route towards both enantiomers of α -amino acids—A model study. *Tetrahedron Asymmetry* **2006**, *17*, 2667–2671. [[CrossRef](#)]
10. Devji, T.; Reddy, C.; Woo, C.; Awale, S.; Kadota, S.; Carrico-Moniz, D. Pancreatic anticancer activity of a novel geranylgeranylated coumarin derivative. *Bioorganic Med. Chem. Lett.* **2011**, *21*, 5770–5773. [[CrossRef](#)]
11. Reddy, N.S.; Mallireddigari, M.R.; Cosenza, S.; Gumireddy, K.; Bell, S.C.; Reddy, E.P.; Reddy, M.R. Synthesis of new coumarin 3-(N-aryl) sulfonamides and their anticancer activity. *Bioorganic Med. Chem. Lett.* **2004**, *14*, 4093–4097. [[CrossRef](#)]
12. Hadjipavlou-Litina, D.J.; Litinas, K.E.; Kontogiorgis, C. The Anti-inflammatory Effect of Coumarin and its Derivatives. *Anti-Inflamm. Anti-Allergy Agents Med. Chem.* **2007**, *6*, 293–306. [[CrossRef](#)]
13. Xue, H.; Lu, X.; Zheng, P.; Liu, L.; Han, C.; Hu, J.; Liu, Z.; Ma, T.; Li, Y.; Wang, L.; et al. Highly Suppressing Wild-Type HIV-1 and Y181C Mutant HIV-1 Strains by 10-Chloromethyl-11-demethyl-12-oxo-calanolide A with Druggable Profile. *J. Med. Chem.* **2010**, *53*, 1397–1401. [[CrossRef](#)]
14. Curini, M.; Epifano, F.; Maltese, F.; Marcotullio, M.C.; Gonzales, S.P.; Rodriguez, J.C. Synthesis of Collinin, an Antiviral Coumarin. *Aust. J. Chem.* **2003**, *56*, 59–60. [[CrossRef](#)]
15. Hwang, C.H.; Jaki, B.U.; Klein, L.L.; Lankin, D.C.; McAlpine, J.B.; Napolitano, J.G.; Fryling, N.A.; Franzblau, S.G.; Cho, S.H.; Stamets, P.E.; et al. Chlorinated Coumarins from the Polypore Mushroom *Fomitopsis officinalis* and Their Activity against *Mycobacterium tuberculosis*. *J. Nat. Prod.* **2013**, *76*, 1916–1922. [[CrossRef](#)] [[PubMed](#)]
16. Arshad, A.; Osman, H.; Bagley, M.C.; Lam, C.K.; Mohamad, S.; Zahariluddin, A.S.M. Synthesis and antimicrobial properties of some new thiazolyl coumarin derivatives. *Eur. J. Med. Chem.* **2011**, *46*, 3788–3794. [[CrossRef](#)] [[PubMed](#)]
17. Laurin, P.; Ferroud, D.; Klich, M.; Dupuis-Hamelin, C.; Mauvais, P.; Lassaigne, P.; Bonnefoy, A.; Musicki, B. Synthesis and in vitro evaluation of novel highly potent coumarin inhibitors of gyrase B. *Bioorganic Med. Chem. Lett.* **1999**, *9*, 2079–2084. [[CrossRef](#)]
18. Tolomelli, A.; Squassabia, F. Peptides and Peptidomimetics in Medicine, Surgery and Biotechnology. *Curr. Med. Chem.* **2006**, *13*, 2449–2466. [[CrossRef](#)]
19. Cottiglia, F.; Loy, G.; Garau, D.; Floris, C.; Casu, M.; Pompei, R.; Bonsignore, L. Antimicrobial evaluation of coumarins and flavonoids from the stems of *Daphne gnidium* L. *Phytomedicine* **2001**, *8*, 302–305. [[CrossRef](#)]
20. Smyth, T.; Ramachandran, V.; Smyth, W. A study of the antimicrobial activity of selected naturally occurring and synthetic coumarins. *Int. J. Antimicrob. Agents* **2009**, *33*, 421–426. [[CrossRef](#)]
21. Kowalczyk, P.; Madej, A.; Paprocki, D.; Szymczak, M.; Ostaszewski, R. Coumarin Derivatives as New Toxic Compounds to Selected K12, R1–R4 *E. coli* Strains. *Materials* **2020**, *13*, 2499. [[CrossRef](#)]
22. Emami, S.; Dadashpour, S. Current developments of coumarin-based anti-cancer agents in medicinal chemistry. *Eur. J. Med. Chem.* **2015**, *102*, 611–630. [[CrossRef](#)]

23. Wilk, M.; Brodzka, A.; Koszelewski, D.; Madej, A.; Paprocki, D.; Żądło-Dobrowolska, A.; Ostaszewski, R. The influence of the isocyanooesters structure on the course of enzymatic Ugi reactions. *Bioorganic Chem.* **2019**, *93*, 102817. [[CrossRef](#)]
24. Wilk, M.; Brodzka, A.; Koszelewski, D.; Samsonowicz-Górski, J.; Ostaszewski, R. Model Studies on the Enzyme-Regulated Diastereodivergent Cascade Passerini Reaction. *Eur. J. Org. Chem.* **2021**, *2021*, 4161–4165. [[CrossRef](#)]
25. Madej, A.; Paprocki, D.; Koszelewski, D.; Żądło-Dobrowolska, A.; Brzozowska, A.; Walde, P.; Ostaszewski, R. Efficient Ugi reactions in an aqueous vesicle system. *RSC Adv.* **2017**, *7*, 33344. [[CrossRef](#)]
26. Paprocki, D.; Koszelewski, D.; Walde, P.; Ostaszewski, R. Efficient Passerini reactions in an aqueous vesicle system. *RSC Adv.* **2015**, *5*, 102828–102835. [[CrossRef](#)]
27. Agban, A.; Ounanian, M.; Luu-Duc, C.; Monget, D. Synthesis of new fluorogenic substrates derivated of 7-amino-4-trifluoromethylcoumarin. Detection of gram-negative bacteria, Streptococci group A and Enterococci. *Ann. Pharm. Fr.* **1990**, *48*, 326–334. [[PubMed](#)]
28. Lukaszewicz, J.; Jachymek, W.; Niedziela, T.; Dzieciatkowska, M.; Lakomska, J.; Międzybrodzki, R.; Fortuna, W.; Szymaniec, S.; Misiuk Hojlo, M.; Lugowski, C. Serological characterization of anti-endotoxin serum directed against the conjugate of oligosaccharide core of *Escherichia coli* type R4 with tetanus toxoid. *FEMS Immunol. Med. Microbiol.* **2003**, *37*, 59–67. [[CrossRef](#)]
29. Nnalue, N.A.; Khan, G.N.; Mustafa, N. Cross-reactivity between six Enterobacteriaceae complete lipopolysaccharide core chemotypes. *J. Med. Microbiol.* **1999**, *48*, 433–441. [[CrossRef](#)] [[PubMed](#)]
30. Heinrichs, D.E.; Yethon, J.A.; Amor, P.A.; Whitfield, C. The assembly system for the outer core portion of R1 and R4 type lipopolysaccharides of *Escherichia coli* the r1 core specific β glucosyltransferase provides a novel attachment site for O-polysaccharides. *J. Biol. Chem.* **1998**, *273*, 29497–29505. [[CrossRef](#)]
31. Amor, K.; Heinrichs, D.E.; Frirdich, E.; Ziebell, K.; Johnson, R.P.; Whitfield, C. Distribution of Core Oligosaccharide Types in Lipopolysaccharides from *Escherichia coli*. *Infect. Immun.* **2000**, *68*, 1116–1124. [[CrossRef](#)] [[PubMed](#)]
32. Appelmelk, B.J.; An, Y.; Hekker, T.A.M.; Thijs, L.G.; MacLaren, D.M.; De Graaf, J. Frequencies of lipopolysaccharide core types in *Escherichia coli* strains from bacteraemic patients. *Microbiology* **1994**, *140*, 1119–1124. [[CrossRef](#)] [[PubMed](#)]
33. Borkowski, A.; Ławniczak, L.; Cłapa, T.; Narożna, D.; Selwet, M.; Pęziak, D.; Markiewicz, B.; Chrzanowski, L. Different antibacterial activity of novel theophylline-based ionic liquids—Growth kinetic and cytotoxicity studies. *Ecotoxicol. Environ. Saf.* **2016**, *130*, 54–64. [[CrossRef](#)]
34. Otaibi, A.A.; Sherwani, S.; Al-Zahrani, S.A.; Alshammari, E.M.; Khan, W.A.; Alsukaibi, A.K.D.; Khan, S.N.; Khan, M.W.A. Biologically Active α -Amino Amide Analogs and $\gamma\delta$ T Cells-A Unique Anticancer Approach for Leukemia. *Front Oncol.* **2021**, *11*, 706586. [[CrossRef](#)] [[PubMed](#)]
35. Krishnamoorthy, K.; Manivannan, G.; Kim, S.J.; Jeyasubramanian, K.; Premanathan, M. Antibacterial activity of MgO nanoparticles based on lipid peroxidation by oxygen vacancy. *J. Nanopart. Res.* **2012**, *14*, 1063. [[CrossRef](#)]
36. Hough-Troutman, W.L.; Smiglak, M.; Griffin, S.; Reichert, W.M.; Mirska, I.; Jodynis-Liebert, J.; Adamska, T.; Nawrot, J.; Stasiewicz, M.; Rogers, R.D.; et al. Ionic liquids with dual biological function: Sweet and anti-microbial, hydrophobic quaternary ammonium-based salts. *New J. Chem.* **2009**, *33*, 26–33. [[CrossRef](#)]
37. Inácio, Â.S.; Domingues, N.; Nunes, A.; Martins, P.; Moreno, M.J.; Estronca, L.; Fernandes, R.; Moreno, A.; Borrego, M.J.; Gomes, J.P.; et al. Quaternary ammonium surfactant structure determines selective toxicity towards bacteria: Mechanisms of action and clinical implications in antibacterial prophylaxis. *J. Antimicrob. Chemother.* **2015**, *71*, 641–654. [[CrossRef](#)]
38. Jurado, J.; Sapparbaev, M.; Matray, T.J.; Greenberg, M.M.; Laval, J. The Ring Fragmentation Product of Thymidine C5-Hydrate When Present in DNA Is Repaired by the *Escherichia coli* Fpg and Nth Proteins†. *Biochemistry* **1998**, *37*, 7757–7763. [[CrossRef](#)]
39. Cussac, C.; Laval, J. Reduction of the Toxicity and Mutagenicity of Aziridine in Mammalian Cells Harboring the *Escherichia coli* fpg Gene. *Nucleic Acids Res.* **1996**, *24*, 1742–1746. [[CrossRef](#)]
40. Kawase, M.; Varu, B.; Shah, A.; Motohashi, N.; Tani, S.; Saito, S.; Debnath, S.; Mahapatra, S.; Dastidar, S.G.; Chakrabarty, A.N. Antimicrobial Activity of New Coumarin Derivatives. *Arzneimittelforschung* **2001**, *51*, 67–71. [[CrossRef](#)]
41. Upadhyay, K.; Manvar, A.; Rawal, K.; Joshi, S.; Trivedi, J.; Chaniyara, R.; Shah, A. Evaluation of Structurally Diverse Benzoazepines Clubbed with Coumarins as *Mycobacterium tuberculosis* Agents. *Chem. Biol. Drug Des.* **2012**, *80*, 1003–1008. [[CrossRef](#)] [[PubMed](#)]
42. Ghosh, A.K. ChemInform Abstract: Potent HIV Protease Inhibitors Incorporating High-Affinity P2-Ligands and (R)-(Hydroxyethylamino)sulfonamide Isostere. *ChemInform* **2010**, *29*, 27. [[CrossRef](#)]
43. Zhao, H.; Neamati, N.; Hong, H.; Mazumder, A.; Wang, S.; Sunder, S.; Milne, G.W.A.; Pommier, Y.; Burke, T.R. Coumarin-Based Inhibitors of HIV Integrase. *J. Med. Chem.* **1997**, *40*, 242–249. [[CrossRef](#)] [[PubMed](#)]
44. Stromberg, Z.R.; Van Goor, A.; Redweik, G.A.J.; Brand, M.J.W.; Wannemuehler, M.J.; Mellata, M. Pathogenic and non-pathogenic *Escherichia coli* colonization and host inflammatory response in a defined microbiota mouse model. *Dis. Models Mech.* **2018**, *11*, dmm035063. [[CrossRef](#)]
45. Larry, K.L.; Tanka, S.K. Therapy of *Helicobacter pylori* Infections: Current Status and Future Directions. In *Annual Reports in Medicinal Chemistry*; Academic Press: Cambridge, MA, USA, 1995; Volume 30, pp. 151–158.
46. Kowalczyk, P.; Trzepizur, D.; Szymczak, M.; Skiba, G.; Kramkowski, K.; Ostaszewski, R. 1,2-Diarylethanol—A New Class of Compounds That Are Toxic to *E. coli* K12, R2–R4 Strains. *Materials* **2021**, *14*, 1025. [[CrossRef](#)]
47. Kowalczyk, P.; Madej, A.; Szymczak, M.; Ostaszewski, R. α -Amidoamids as New Replacements of Antibiotics—Research on the Chosen K12, R2–R4 *E. coli* Strains. *Materials* **2020**, *13*, 5169. [[CrossRef](#)]

48. Kowalczyk, P.; Borkowski, A.; Czerwonka, G.; Cłapa, T.; Cieśla, J.; Misiewicz, A.; Borowiec, M.; Szala, M. The microbial toxicity of quaternary ammonium ionic liquids is dependent on the type of lipopolysaccharide. *J. Mol. Liq.* **2018**, *266*, 540–547. [[CrossRef](#)]
49. Borkowski, A.; Kowalczyk, P.; Czerwonka, G.; Cieśla, J.; Cłapa, T.; Misiewicz, A.; Szala, M.; Drabik, M. Interaction of quaternary ammonium ionic liquids with bacterial membranes—Studies with *Escherichia coli* R1–R4-type lipopolysaccharides. *J. Mol. Liq.* **2017**, *246*, 282–289. [[CrossRef](#)]
50. Kowalczyk, P.; Gawdzik, B.; Trzepizur, D.; Szymczak, M.; Skiba, G.; Raj, S.; Kramkowski, K.; Lizut, R.; Ostaszewski, R. δ -Lactones—A New Class of Compounds That Are Toxic to *E. coli* K12 and R2–R4 Strains. *Materials* **2021**, *14*, 2956. [[CrossRef](#)]
51. Dissanayake, D.R.; Wijewardana, T.G.; Gunawardena, G.A.; Poxton, I.R. Distribution of lipopolysaccharide core types among avian pathogenic *Escherichia coli* in relation to the major phylogenetic groups. *Vet. Microbiol.* **2008**, *132*, 355–363. [[CrossRef](#)]
52. Maciejewska, A.; Kaszowska, M.; Jachymek, W.; Lugowski, C.; Lukaszewicz, J. Lipopolysaccharide-linked Enterobacterial Common Antigen (ECA_{LPS}) Occurs in Rough Strains of *Escherichia coli* R1, R2, and R4. *Int. J. Mol. Sci.* **2020**, *21*, 6038. [[CrossRef](#)] [[PubMed](#)]
53. Prost, M.E.; Prost, R. Basic parameters of evaluation of the effectiveness of antibiotic therapy. *OphthaTherapy* **2017**, *4*, 233–236. [[CrossRef](#)]
54. D'Souza, L.J.; Gigant, B.; Knossow, M.; Green, B.S. Remarkable remote chiral recognition in a reaction mediated by a catalytic antibody. *J. Am. Chem. Soc.* **2002**, *124*, 2114–2115. [[CrossRef](#)] [[PubMed](#)]
55. Castonguay, R.; Lherbet, C.; Keillor, J.W. Mapping of the active site of rat kidney γ -glutamyl transpeptidase using activated esters and their amide derivatives. *Bioorganic Med. Chem.* **2002**, *10*, 4185–4191. [[CrossRef](#)]
56. Vrinceanu, D.; Dumitru, M.; Stefan, A.; Neagos, A.; Musat, G.; Nica, E.A. Severe DRESS syndrome after carbamazepine intake in a case with multiple addictions: A case report. *Exp. Ther. Med.* **2020**, *20*, 2377–2380. [[CrossRef](#)]
57. Tamayo, M.; Santiso, R.; Gosálvez, J.; Bou, G.; del Carmen Fernandez, M.; Fernández, J.L. Cell wall active antibiotics reduce chromosomal DNA fragmentation by peptidoglycan hydrolysis in *Staphylococcus aureus*. *Arch. Microbiol.* **2012**, *194*, 967–975. [[CrossRef](#)]
58. Opoku-Temeng, C.; Onyedibe, K.I.; Aryal, U.K.; Sintim, H.O. Proteomic analysis of bacterial response to a 4-hydroxybenzylidene indolinone compound, which re-sensitizes bacteria to traditional antibiotics. *J. Proteom.* **2019**, *202*, 103368. [[CrossRef](#)]
59. Osano, E.; Arakawa, Y.; Wacharotayankun, R.; Ohta, M.; Horii, T.; Ito, H.; Yoshimura, F.; Kato, N. Molecular characterization of an enterobacterial metallo beta-lactamase found in a clinical isolate of *Serratia marcescens* that shows imipenem resistance. *Antimicrob. Agents Chemother.* **1994**, *38*, 71–78. [[CrossRef](#)]